

Exact Solution to the Haldane-BCS-Hubbard Model Along the Symmetric Lines: Interaction Induced Topological Phase Transition

Jian-Jian Miao,¹ Dong-Hui Xu,² Long Zhang,^{1,3,*} and Fu-Chun Zhang^{1,3,†}

¹*Kaoli Institute for Theoretical Sciences and CAS Center for Excellence in Topological Quantum Computation, University of Chinese Academy of Sciences, Beijing 100190, China*

²*Department of Physics, Hubei University, Wuhan 430062, China*

³*Physical Science Laboratory, Huairou National Comprehensive Science Center, Beijing 101400, China*

(Dated: May 19, 2022)

We propose a Haldane-BCS-Hubbard model on a honeycomb lattice, which is composed of two copies of the Haldane model of the quantum anomalous Hall effect, an equal-spin pairing term and an onsite Hubbard interaction term. For any interaction strength, this model is exactly solvable along the symmetric line where the hopping and pairing amplitudes are equal to each other. The ground state of the Haldane-BCS-Hubbard model is a topological superconducting state when the interaction is weak. A strong enough interaction will cause the spontaneous breaking of Z_2 symmetry and result in a topologically trivial antiferromagnetic state with staggered magnetization in the y -direction.

I. INTRODUCTION

The interplay of topology and correlations can lead to novel phases and phase transitions in condensed matter systems. A canonical example is the exactly solvable Kitaev honeycomb model¹, whose ground states are quantum spin liquid and the phase transition between Abelian and non-Abelian phases can be characterized by the spectral Chern number. An exactly solvable model in strongly correlated systems is enlightening without the flaws of various approximation methods, and can serve as a benchmark for further study. Recently, Chen et. al.² generalized the Kitaev honeycomb model to spinful fermion models. Later Ezawa³ studied the exactly solvable BCS-Hubbard model on the honeycomb lattice by including the Kane-Mele spin-orbit coupling (SOC). However, an infinitesimal Hubbard interaction U will destroy the topological superconducting state due to the spontaneous time reversal symmetry breaking in³. It is desirable to find an exactly solvable model can give rise to topological superconducting states in the presence of finite repulsive interaction.

In this paper, we investigate the Haldane-BCS-Hubbard model on a honeycomb lattice in(1). Along the symmetric lines where the hopping amplitude equals the pairing gap, the model is exactly solvable and reduces to the Falicov-Kimball model⁴ with one species of Majorana fermions fully localized. There is an interaction induced topological phase transition at finite Hubbard U . The phase transition can be characterized by the change of the spectral Chern number.

The paper is organized as follows: In section II, we introduce the Haldane-BCS-Hubbard model. Then we show the exact solvability along the symmetric lines in section III. We analyze the symmetry of the model in section IV and introduce the composite fermion representation in section V for later convenience. In section VI, we study the noninteracting limit of the model and give the phase diagram. In section VII, we study the model

along the symmetric lines and show the interaction induced topological phase transition. We summarize the results and propose the possible realization of the model in section VIII.

II. MODEL HAMILTONIAN

In this section, we introduce the Haldane-BCS-Hubbard model we study. The Hamiltonian of the model consists of three parts and can be expressed as follows

$$H = H_{hop} + H_{pair} + H_{int} \quad (1)$$

where H_{hop} describes the electron hopping terms, which is a spinful generalization of the Haldane model^{5,6}, H_{pair} describes the equal spin pairing (ESP) terms, and H_{int}

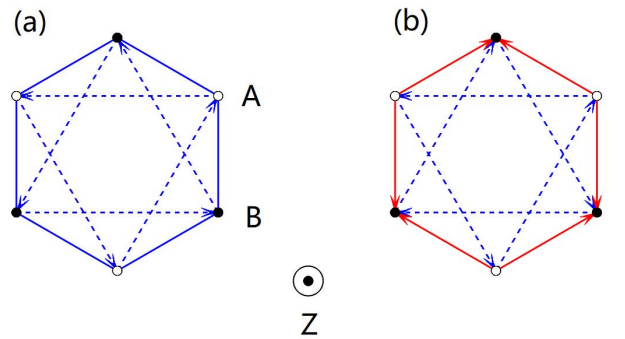


FIG. 1: (Color online) (a) The signs ν_{ij} of the spin-orbit coupling terms. Along the direction of the dashed lines $\nu_{ij} = +1$, while along the reversed direction $\nu_{ij} = -1$. (b) The signs of the nearest and next-nearest neighbor pairing terms. Along the direction of the red (dashed) lines the signs of Δ_1 (Δ_2) are +1, while along the reversed direction they are -1. White sites A and black sites B are the two sublattices. z -direction points outward the plane.

describes the on-site Hubbard interactions. They are given by

$$H_{hop} = t_1 \sum_{\langle ij \rangle_s} c_{is}^\dagger c_{js} - t_2 \sum_{\langle\langle ij \rangle\rangle_s} i\nu_{ij} c_{is}^\dagger c_{js} \quad (2)$$

$$H_{pair} = \Delta_1 \sum_{\langle ij \rangle_s} c_{is}^\dagger c_{js}^\dagger + \Delta_2 \sum_{\langle\langle ij \rangle\rangle_s} i\nu_{ij} \epsilon_i c_{is}^\dagger c_{js}^\dagger + h.c. \quad (3)$$

$$H_{int} = U \sum_i (n_{i\uparrow} - \frac{1}{2})(n_{i\downarrow} - \frac{1}{2}) \quad (4)$$

where c_{is} (c_{is}^\dagger) annihilates (creates) an electron at site i with spin $s = \uparrow, \downarrow$ pointing in the z -direction. $\langle ij \rangle$ and $\langle\langle ij \rangle\rangle$ denote the nearest and next-nearest neighbor sites. t_1 is the nearest neighbor hopping matrix element and t_2 is the SOC strength. The sign $\nu_{ij} = \text{sign}(\hat{d}_1 \times \hat{d}_2)_z = \pm 1$, where $\hat{d}_{1,2}$ are the vectors along the two bonds constituting the next-nearest neighbors. The signs ν_{ij} are shown in FIG. 1. Δ_1 and Δ_2 are the nearest and next-nearest neighbor ESP potential respectively. $\epsilon_i = \pm 1$ for sublattices A and B respectively. The signs of $\Delta_{1,2}$ are shown in FIG. 1. $n_{is} = c_{is}^\dagger c_{is}$ is the fermionic number operator for spin s . U is the strength of on-site Hubbard interaction.

III. EXACT SOLVABILITY

In this section, we shall show the exact solvability of the Haldane-BCS-Hubbard model along the symmetric

lines

$$t_1 = \Delta_1, \quad t_2 = \Delta_2. \quad (5)$$

The Haldane-BCS-Hubbard model is not exactly solvable in general. However, similar to the BCS-Hubbard model², we find this model can be solved exactly along the symmetric lines. The exact solvability of the model becomes manifest in the Majorana fermion representation. As the system contains two sublattices, we use r to denote the unit cell and $c_{rs\epsilon}$ to denote the annihilation operator with spin s at unit cell r in sublattice $\epsilon = A, B$. We then decompose the complex fermion operators $c_{rs\epsilon}$ into Majorana fermion operators $\eta_{rs\epsilon}$ and $\gamma_{rs\epsilon}$ as follows

$$\begin{aligned} c_{rsA} &= \eta_{rsA} + i\gamma_{rsA} \\ c_{rsB} &= \gamma_{rsB} + i\eta_{rsB} \end{aligned} \quad (6)$$

Note the decomposition is opposite for the two sublattices. The Hamiltonian in the Majorana fermion representation becomes

$$\begin{aligned} H_0 &= \delta_1 \sum_{rs} i\eta_{rsA}\eta_{rsB} + i\eta_{rsA}\eta_{r+a_1sB} + i\eta_{rsA}\eta_{r+a_2sB} \\ &\quad - \tilde{t}_1 \sum_{rs} i\gamma_{rsA}\gamma_{rsB} + i\gamma_{rsA}\gamma_{r+a_1sB} + i\gamma_{rsA}\gamma_{r+a_2sB} \\ &\quad - \delta_2 \sum_{rs\epsilon} \epsilon (i\eta_{rs\epsilon}\eta_{r+a_1s\epsilon} + i\eta_{rs\epsilon}\eta_{r-a_1+a_2s\epsilon} + i\eta_{rs\epsilon}\eta_{r-a_2s\epsilon}) \\ &\quad - \tilde{t}_2 \sum_{rs\epsilon} \epsilon (i\gamma_{rs\epsilon}\gamma_{r+a_1s\epsilon} + i\gamma_{rs\epsilon}\gamma_{r-a_1+a_2s\epsilon} + i\gamma_{rs\epsilon}\gamma_{r-a_2s\epsilon}) \\ H_{int} &= U \sum_{r\epsilon} 2i\eta_{r\uparrow\epsilon}\gamma_{r\uparrow\epsilon} 2i\eta_{r\downarrow\epsilon}\gamma_{r\downarrow\epsilon} \end{aligned} \quad (7)$$

where $H_0 = H_{hop} + H_{pair}$ and $\delta_1 = 2(t_1 - \Delta_1)$, $\delta_2 = 2(t_2 - \Delta_2)$, $\tilde{t}_1 = 2(t_1 + \Delta_1)$, $\tilde{t}_2 = 2(t_2 + \Delta_2)$. $a_1 = a\left(\frac{1}{2}, \frac{\sqrt{3}}{2}\right)$ and $a_2 = a\left(-\frac{1}{2}, \frac{\sqrt{3}}{2}\right)$ are the two basis vectors. Note the η Majorana fermions disappear in the noninteracting Hamiltonian H_0 along the symmetric lines $\delta_1 = \delta_2 = 0$. In the following, we shall focus on the symmetric line. We define $\hat{D}_{r\epsilon} = 4i\eta_{r\uparrow\epsilon}\eta_{r\downarrow\epsilon}$. It is easy to prove that $[\hat{D}_{r\epsilon}, H] = 0$. Thus $\hat{D}_{r\epsilon}$ are constants of mo-

tion. Since $\hat{D}_{r\epsilon}^2 = 1$, we can replace the operators $\hat{D}_{r\epsilon}$ by its eigenvalues $D_{r\epsilon} = \pm 1$. The Hubbard interaction becomes

$$H_{int} = -U \sum_{r\epsilon} D_{r\epsilon} i\gamma_{r\uparrow\epsilon}\gamma_{r\downarrow\epsilon} \quad (8)$$

The total Hilbert space can be divided into different sectors characterized by the sets of $\{D_{r\epsilon}\}$. Within each sector, the Hamiltonian contains only quadratic γ Majorana fermions and can be solved exactly.

IV. SYMMETRY

Symmetry plays an important role in the following analysis. In this section, we shall analyze the various symmetry of the Haldane-BCS-Hubbard model. The fermion operators transform as $Cc_{is}C^{-1} = \epsilon_i c_{is}^\dagger$ under the particle-hole symmetry (PHS). It is obvious that the Hamiltonian has the PHS⁷. The time reversal symmetry (TRS) operator for spinful system is $T = i\sigma^y K$, where K denotes the complex conjugation and $T^2 = -1$. The fermion operators transform as $Tc_{is}T^{-1} = \sum_{s'} (i\sigma^y)_{ss'} c_{is'}$ under TRS. Just as in the Haldane model, the SOC terms break the TRS explicitly. The sublattice symmetry (SLS) can be implemented by the bond centered inversion operator I . The signs shown in FIG. 1 indicate H_{pair} breaks the SLS. With SOC and ESP terms, the Hamiltonian does not preserve the $SU(2)$ spin rotation symmetry.

V. COMPOSITE FERMION REPRESENTATION

In this section, we introduce the composite fermion representation. These composite fermions form the quasiparticles for the Haldane-BCS-Hubbard model. We

define the composite fermions as in Ref.²

$$\begin{aligned} d_{r2\epsilon} &= \eta_{r\uparrow\epsilon} + i\epsilon\eta_{r\downarrow\epsilon} \\ d_{r1\epsilon} &= \gamma_{r\uparrow\epsilon} - i\epsilon\gamma_{r\downarrow\epsilon} \end{aligned} \quad (9)$$

The physical meaning of the composite fermions becomes clear by introducing the fermion operators pointing in the $\pm y$ -direction as follows

$$c_{r\pm\epsilon}^\dagger = \frac{1}{\sqrt{2}} \left(c_{r\uparrow\epsilon}^\dagger \pm i c_{r\downarrow\epsilon}^\dagger \right) \quad (10)$$

We express d composite fermions in terms of c fermion operators

$$\begin{aligned} d_{r2A} &= \frac{c_{r-A} + c_{r+A}^\dagger}{\sqrt{2}}, d_{r2B} = \frac{c_{r+B} - c_{r-B}^\dagger}{\sqrt{2}i} \\ d_{r1A} &= \frac{c_{r+A} - c_{r-A}^\dagger}{\sqrt{2}i}, d_{r1B} = \frac{c_{r-B} + c_{r+B}^\dagger}{\sqrt{2}} \end{aligned} \quad (11)$$

which are equal-weight superposition of particle and hole of c fermion operators. Thus d composite fermions are chargeless. We also note d_{r1A} and d_{r2B} (d_{r2A} and d_{r1B}) carry spin-1/2 pointing in the y ($-y$)-direction. We write the Hamiltonian in the composite fermion representation

$$\begin{aligned} H_0 &= \frac{i\delta_1}{2} \sum_r d_{r2A}^\dagger d_{r2B}^\dagger + d_{r2A}^\dagger d_{r+a_12B}^\dagger + d_{r2A}^\dagger d_{r+a_22B}^\dagger \\ &\quad - \frac{i\tilde{t}_1}{2} \sum_r d_{r1A}^\dagger d_{r1B}^\dagger + d_{r1A}^\dagger d_{r+a_11B}^\dagger + d_{r1A}^\dagger d_{r+a_21B}^\dagger \\ &\quad - \frac{i\delta_2}{2} \sum_{r\epsilon} \epsilon \left(d_{r2\epsilon}^\dagger d_{r+a_12\epsilon} + d_{r2\epsilon}^\dagger d_{r-a_1+a_22\epsilon} + d_{r2\epsilon}^\dagger d_{r-a_22\epsilon} \right) \\ &\quad - \frac{i\tilde{t}_2}{2} \sum_{r\epsilon} \epsilon \left(d_{r1\epsilon}^\dagger d_{r+a_11\epsilon} + d_{r1\epsilon}^\dagger d_{r-a_1+a_21\epsilon} + d_{r1\epsilon}^\dagger d_{r-a_21\epsilon} \right) \\ &\quad + h.c. \\ H_{int} &= U \sum_{r\epsilon} \left(n_{r2\epsilon} - \frac{1}{2} \right) \left(n_{r1\epsilon} - \frac{1}{2} \right) \end{aligned} \quad (12)$$

where $n_{r\alpha\epsilon} = d_{r\alpha\epsilon}^\dagger d_{r\alpha\epsilon}$ with $\alpha = 1, 2$. Thus the original system can be viewed as two species of d composite fermions with nearest neighbor pairing, next-nearest neighbor SOC, and they interact with on-site Hubbard U . Note the Hamiltonian H has the dual symmetry under the dual mapping $d_{r1\epsilon} \leftrightarrow d_{r2\epsilon}$ (or $\eta_{rse} \leftrightarrow \gamma_{rse}$), with parameters changing as $\delta_1 \leftrightarrow -\tilde{t}_1$, $\delta_2 \leftrightarrow \tilde{t}_2$. Thus the Hamiltonian H has a self-dual point $t_1 = \Delta_2 = 0$, even with the Hubbard interaction U . In the following, we shall analyze the properties of the Haldane-BCS-Hubbard model in terms of d composite fermions.

VI. NONINTERACTING LIMIT: HALDANE-BCS MODEL

In this section, we analyze the noninteracting limit of the Haldane-BCS-Hubbard model. At $U = 0$, the model reduces to the Haldane-BCS model. Note the Hamiltonian H_0 is decoupled for two species of d composite fermions $H_0 = H_1 + H_2$, where H_α contains d_α composite fermions only. The Hamiltonian H_0 is uniform and we can perform the Fourier transformation to obtain the

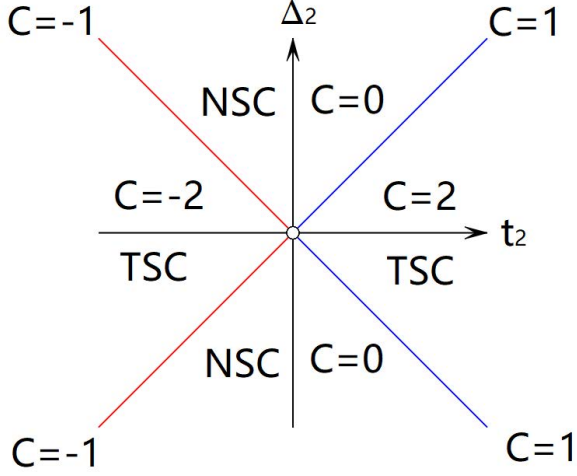


FIG. 2: (Color online) The phase diagram of the Haldane-BCS model with $t_1 = 2\Delta_1 = 1$. TSC denotes the topological superconducting state with Chern number $C = \pm 2$. NSC denotes the trivial superconducting state with Chern number $C = 0$. The blue (red) lines denote one species of d composite fermions is gapless and another species is in TSC with Chern number $C = 1$ ($C = -1$).

spectrum. The Fourier transformation is defined as

$$d_{r\alpha\epsilon} = \frac{1}{\sqrt{N}} \sum_k e^{ik \cdot r} d_{k\alpha\epsilon} \quad (13)$$

We also define the spinor as $\psi_{k\alpha}^\dagger = (d_{k\alpha A}^\dagger, d_{-k\alpha B}^\dagger)$, the Hamiltonian H_α can be written in the form of

$$H_\alpha = \sum_k \psi_{k\alpha}^\dagger h_\alpha(k) \psi_{k\alpha} \quad (14)$$

where

$$h_\alpha(k) = \vec{T}_\alpha(k) \cdot \vec{\sigma} \quad (15)$$

$\vec{\sigma} = (\sigma^x, \sigma^y, \sigma^z)$ are the Pauli matrices and $\vec{T}_1(k)$ are given by

$$\begin{aligned} T_1^x(k) &= \frac{\tilde{t}_1}{2} (\sin k \cdot e_1 + \sin k \cdot e_2 + \sin k \cdot e_3) \\ T_1^y(k) &= \frac{\tilde{t}_1}{2} (\cos k \cdot e_1 + \cos k \cdot e_2 + \cos k \cdot e_3) \\ T_1^z(k) &= \tilde{t}_2 (\sin k \cdot a_1 - \sin k \cdot (a_1 - a_2) - \sin k \cdot a_2) \end{aligned} \quad (16)$$

where $e_1 = a \left(0, -\frac{1}{\sqrt{3}}\right)$, $e_2 = a \left(\frac{1}{2}, \frac{1}{2\sqrt{3}}\right)$ and $e_3 = a \left(-\frac{1}{2}, \frac{1}{2\sqrt{3}}\right)$ are the three vectors of nearest neighbor bonds. $\vec{T}_2(k)$ can be obtained by the dual mapping $d_{r1\epsilon} \rightarrow d_{r2\epsilon}$ with parameters changing as $\tilde{t}_1 \rightarrow -\delta_1$ and $\tilde{t}_2 \rightarrow \delta_2$. The energy dispersions read $E_\alpha(k) = \pm |\vec{T}_\alpha(k)|$, which

form reflects the PHS of the Hamiltonian. The ground state is unique with all the negative energy levels of both d composite fermions occupied. The system is gapped for nonzero \tilde{t}_1, \tilde{t}_2 and δ_1, δ_2 .

The noninteracting Hamiltonian H_0 describes two components Haldane model with ESP at half-filling. According to the symmetry analysis in section IV, the system falls into the category of topological superconductor (SC) belonging to class D^8 . The topological invariant is characterized by the total Chern number⁹ $C = C_1 + C_2$, where C_α denotes the Chern number of d_α composite fermions. We calculate the Chern number¹⁰ and find

$$C_1 = \text{sign}(\tilde{t}_2), \quad (17)$$

$$C_2 = \text{sign}(\delta_2), \quad (18)$$

where $\text{sign}(x) = \lim_{\epsilon \rightarrow 0} \frac{x}{\sqrt{x^2 + \epsilon^2}}$ is the sign function. Thus the total Chern number is given by

$$C = \text{sign}(t_2 + \Delta_2) + \text{sign}(t_2 - \Delta_2) \quad (19)$$

which indicates the topological phase transition at $t_2 = \pm \Delta_2$. Accordingly the gap closes for d_1 (d_2) composite fermions at $t_2 = -\Delta_2$ ($t_2 = \Delta_2$). The phase diagram of Haldane-BCS model is shown in FIG. 2. For $|t_2| > |\Delta_2|$, the system is in the topological SC state with total Chern number $C = \pm 2$. For $|t_2| < |\Delta_2|$, the system is in the trivial SC state with total Chern number $C = 0$. At the critical lines $t_2 = \pm \Delta_2$, one species of d composite fermions is gapless and another species is in the topological SC state with Chern number $C = \pm 1$. The origin is a gapless multicritical point.

The topological phase transition can be understood via the bulk-edge corresponding. Except at the critical lines, each species of d composite fermions has nonzero Chern number, i.e. in the topological SC state with single chiral edge state. For $|t_2| > |\Delta_2|$, both edge states carry the same chirality and the system is in the topological SC state with two chiral edge states. However for $|t_2| < |\Delta_2|$, two edge states with opposite chirality cancel with each other. The system becomes a trivial SC state with total Chern number $C = 0$. We plot the energy spectrum of d_2 composite fermions with different sign of δ_2 in Fig. 3 and find in both cases the system has single chiral edge state on each edge. Due to sign change of δ_2 , the wavefunctions of the edge states localize on opposite edges, which indicates the chirality of the edge states is changed. This is consistent with the sign change of Chern number of d_2 composite fermions. At the critical lines $t_2 = \pm \Delta_2$, one chiral edge state merges into the bulk and the system becomes a gapless topological SC state with single chiral edge state. The topological phase transition can also be revealed by another dual mapping $\eta_\epsilon \rightarrow \epsilon \eta_{\bar{\epsilon}}$ ($\gamma_\epsilon \rightarrow \epsilon \gamma_{\bar{\epsilon}}$), where $\bar{\epsilon}$ is the different sublattice of ϵ . The Hamiltonian has the dual symmetry with parameters changing as $t_2 \leftrightarrow \Delta_2$ ($t_2 \leftrightarrow -\Delta_2$). The topological phase transition happens exactly at the self-dual point $t_2 = \pm \Delta_2$. Similar duality relating topological and trivial phases has been discovered in the interacting Kitaev chain¹¹. If we

employ the BdG formalism¹² and use the Nambu spinor $\Psi_{k\alpha}^\dagger = (d_{k\alpha A}^\dagger, d_{k\alpha B}^\dagger, d_{-k\alpha A}, d_{-k\alpha B})$, the above analysis is still valid except the Chern numbers should be multiplied by 2 and each chiral edge state becomes two chiral Majorana edge states.

VII. HALDANE-BCS-HUBBARD MODEL ALONG SYMMETRIC LINES

In this section, we analyze the Haldane-BCS-Hubbard model along the symmetric lines $\delta_1 = \delta_2 = 0$. In terms of d composite fermions language, the d_2 fermions are completely localized (or form the completely flat bands in the band theory language³). The Hamiltonian effectively reduces to the Falicov-Kimball model with only one species of mobile d composite fermions

$$\begin{aligned}
H_s = & -\frac{i\tilde{t}_1}{2} \sum_r d_{r1A}^\dagger d_{r1B}^\dagger + d_{r1A}^\dagger d_{r+a_11B}^\dagger + d_{r1A}^\dagger d_{r+a_21B}^\dagger + h.c. \\
& -\frac{i\tilde{t}_2}{2} \sum_{r\epsilon} \epsilon \left(d_{r1\epsilon}^\dagger d_{r+a_11\epsilon} + d_{r1\epsilon}^\dagger d_{r-a_1+a_21\epsilon} + d_{r\epsilon}^\dagger d_{r-a_21\epsilon} \right) + h.c. \\
& \pm \frac{U}{2} \sum_{r\epsilon} \left(n_{r1\epsilon} - \frac{1}{2} \right)
\end{aligned} \tag{20}$$

where $D_{r\epsilon} = 2\epsilon(n_{r2\epsilon} - \frac{1}{2}) = \pm\epsilon$. The d_2 composite fermions form the background Z_2 charge fields. Note the Hamiltonian is symmetric with respect to the Hubbard U along the symmetric lines. As the ground state sectors are translation invariant, we can perform the Fourier transformation and the Hamiltonian H_s can also be written in the form of

$$H_s = \sum_k \psi_{k1}^\dagger h_s(k) \psi_{k1} \tag{21}$$

where

$$h_s(k) = \vec{T}_s(k) \cdot \vec{\sigma} \tag{22}$$

with $T_s^x = T_1^x$, $T_s^y = T_1^y$ and $T_s^z = T_1^z \pm \frac{U}{2}$. The energy dispersion reads $E_s(k) = \pm|\vec{T}_s(k)|$, which is gapped except at $U = \pm 3\sqrt{3}\tilde{t}_2$. The quasiparticle excitations are the chargeless and spin-1/2 d_1 composite fermions. Even with the Hubbard interactions, we can define the spectral Chern number in terms of these quasiparticles along the symmetric lines. The spectral Chern number is given by

$$C_s = \frac{1}{2} \left[\text{sign} \left(3\sqrt{3}\tilde{t}_2 - U \right) + \text{sign} \left(3\sqrt{3}\tilde{t}_2 + U \right) \right] \tag{23}$$

Thus there is a topological phase transition at $U = \pm 3\sqrt{3}\tilde{t}_2$ and the gap closes at this point accordingly.

As the total Hilbert space is divided into different sectors characterized by the sets of $\{D_{r\epsilon}\}$, we first determine the ground state sector. Within each sector, the ground state energy is by summing all the negative energy levels. The ground state sector is determined by the set of $\{D_{r\epsilon}\}$ with minimal ground state energy. We traverse all the 2^N sectors numerically for small lattice size and find the ground state sectors are $\{D_{r\epsilon} = \pm\epsilon\}$. We also note the sectors $\{D_{r\epsilon} = \pm 1\}$ have the maximal ground state energy. For large lattice size, we randomly choose the sector $\{D_{r\epsilon}\}$ and find its ground state energy always falls between the sectors $\{D_{r\epsilon} = \pm\epsilon\}$ and $\{D_{r\epsilon} = \pm 1\}$. Thus we conclude the ground state sectors are $\{D_{r\epsilon} = \pm\epsilon\}$. The ground states are uniform with two-fold degeneracy.

Within the ground state sectors, the Hamiltonian of the Haldane-BCS-Hubbard model along the symmetric lines reduces to

This topological phase transition can be understood easily in terms of d_1 composite fermions. Within each sector, the Hubbard interactions act as chemical potential terms. For small U , the system is in the weak pairing region and topological. While for large U , the system is in the strong pairing region and becomes topologically trivial^{13,14}. The topological phase transition is due to the competition between the SOC and Hubbard interactions. This mechanism is remarkably different from the Kane-Mele-BCS-Hubbard model studied in Ref.³, where infinitesimal U renders the topological SC state into trivial. The reason is that its topological SC state is protected by the TRS, while the Hubbard interaction cause TRS breaking terms and mix different spin components within each sector as $Ti\gamma_{\uparrow\epsilon}\gamma_{\downarrow\epsilon}T^{-1} = -i\gamma_{\uparrow\epsilon}\gamma_{\downarrow\epsilon}$. Thus its phase transition is due to spontaneous TRS breaking without gap closing and happens at infinitesimal U . In the Haldane-BCS-Hubbard model along the symmetric lines, the topological phase transition happens at finite U , which clearly manifests the competition of topology and correlations.

We study the properties of ground states with the aid of symmetry analysis. Even though the Hamiltonian does not have the inversion symmetry I , we note it has the combined symmetry \tilde{I} of bond centered inversion I plus gauge transformation $c_{r\epsilon} \rightarrow \sum_{s'} (i\sigma^z)_{ss'} c_{rs'\epsilon}$. The two

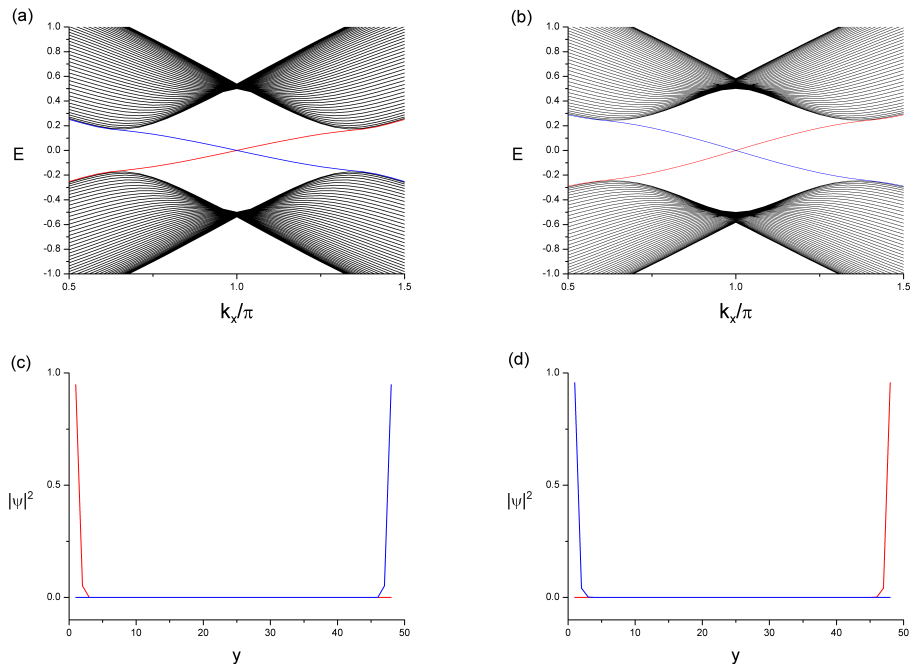


FIG. 3: (Color online) (a) and (b) Energy spectrum of d_2 composite fermions in a cylinder geometry with periodic boundary conditions in the x -direction. The calculations is done for $t_1 = 2\Delta_1 = 1$, $t_2 = 0.1$ with lattice size 48×48 . The system has single chiral edge state on each edge for $\Delta_2 = 0$ in (a) and $\Delta_2 = 0.25$ in (b), but with the opposite chirality. (c) and (d) are the real space wavefunction distribution of the edge states corresponding to (a) and (b).

degenerate ground states are transformed to each other by the symmetry \tilde{I} . Thus the ground states spontaneously break the Z_2 symmetry \tilde{I} for nonzero U . We define the transverse magnetism in the y -direction as the order parameter²

$$m_{r\epsilon}^y = \frac{1}{2} \langle c_{r+\epsilon}^\dagger c_{r+\epsilon} - c_{r-\epsilon}^\dagger c_{r-\epsilon} \rangle \quad (24)$$

which transforms odd under the symmetry \tilde{I} . We calculate the transverse magnetism via the operator identity

$$c_{r+\epsilon}^\dagger c_{r+\epsilon} - c_{r-\epsilon}^\dagger c_{r-\epsilon} = \epsilon \left(d_{r1\epsilon}^\dagger d_{r1\epsilon} - d_{r2\epsilon}^\dagger d_{r2\epsilon} \right) \quad (25)$$

For comparison, we find $\langle d_{r\alpha\epsilon}^\dagger d_{r\alpha\epsilon} \rangle = \frac{1}{2}$ in the noninteracting limit. Thus the ground state is nonmagnetic for Haldane-BCS model. For nonzero U , we have

$$\begin{aligned} \langle d_{r1\epsilon}^\dagger d_{r1\epsilon} \rangle &= \frac{1}{N} \sum_k \left(\frac{1}{2} \mp \frac{T_s^z(k)}{2E_s(k)} \right) \\ \langle d_{r2\epsilon}^\dagger d_{r2\epsilon} \rangle &= \frac{1}{2} + \frac{\epsilon D_{r\epsilon}}{2} \end{aligned} \quad (26)$$

The order parameter is given by

$$m_{r\epsilon}^y = \pm \frac{\epsilon}{2} \left(\frac{1}{2} + \frac{1}{N} \sum_k \frac{T_s^z(k)}{2E_s(k)} \right) \quad (27)$$

Thus the ground states have staggered magnetism and are antiferromagnetic for nonzero U . The transverse

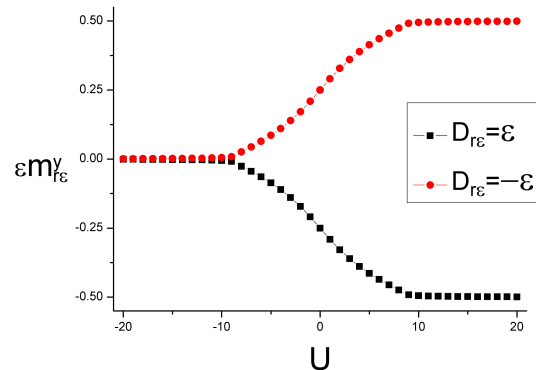


FIG. 4: (Color online) The transverse magnetism in the y -direction. The parameters are $t_1 = 1$ and $t_2 = \sqrt{3}$.

magnetism shown in FIG. 4 indicates the Z_2 symmetry \tilde{I} is spontaneously breaking. In the limit $U \rightarrow \infty$, there is only one electron per site and the spin tend to be fully polarized. Accordingly we have $m_{r\epsilon}^y \rightarrow \pm \frac{\epsilon}{2}$. In the limit $U \rightarrow -\infty$, there are zero or two electrons per site with vanishing spin polarization. Accordingly we have $m_{r\epsilon}^y \rightarrow 0$.

VIII. DISCUSSION AND EXPERIMENTAL REALIZATION

In this paper, we study the Haldane-BCS-Hubbard model. We find this model can be solved exactly along the symmetric lines. In the noninteracting limit, the Haldane-BCS model has topological phase transitions at the self-dual points. The topological phase transition are revealed by the bulk-edge corresponding. Along the symmetric lines, we find the model reduces to the Falicov-Kimball model. There is an interaction induced topological phase transition due to the competition between SOC and Hubbard interactions. With nonzero Hubbard U , the ground states spontaneously break the combined inversion symmetry and have staggered transverse magnetism in the y -direction.

The Haldane model has already been realized in the cold atoms system¹⁵. Actually we can view our model as bilayer of Haldane models. The spin index s can be viewed as upper lay index with $s = \uparrow$ for upper layer and $s = \downarrow$ for bottom layer. We can introduce the ESP and tune the on-site interaction Hubbard U between two layers in cold atoms system. We expect the interaction induced topological phase transition can be observed in cold atoms system.

IX. ACKNOWLEDGEMENT

JJM acknowledges the discussion with Yi Zhou. JJM is supported by China Postdoctoral Science Foundation

(Grant No.2017M620880) and the National Natural Science Foundation of China (Grant No.1184700424). DHX is supported by the National Natural Science Foundation of China (Grant No. 11704106) and the Scientific Research Project of Education Department of Hubei Province (Grant No. Q20171005). DHX also acknowledges the support of the Chutian Scholars Program in Hubei Province. LZ is supported by National Key R&D Program of China (No. 2018YFA0305800) and National Natural Science Foundation of China (No. 11804337). Work at UCAS is also supported by Strategic Priority Research Program of CAS (No. XDB28000000), and Beijing Municipal Science & Technology Commission (No. Z181100004218001). FCZ is supported by National Science Foundation of China (Grant No.11674278), National Basic Research Program of China (No.2014CB921203), and the CAS Center for Excellence in Topological Quantum Computation.

X. NOTE ADDED

During the preparation of this work, we find a similar work on arXiv¹⁶, which also studies the extension of the BCS-Hubbard model² (now named as Majorana Falicov-Kimball Model) more thorough.

* Electronic address: longzhang@ucas.ac.cn

† Electronic address: fuchun@ucas.ac.cn

¹ A. Kitaev, Ann. Phys. (Amsterdam) 321, 2 (2006).

² Z. Chen, X. Li and T. K. Ng, Phys. Rev. Lett. 120, 046401 (2018).

³ M. Ezawa, Phys. Rev. B 97, 241113(R) (2018).

⁴ L. M. Falicov, and J. C. Kimball, Phys. Rev. Lett. 22, 997 (1969).

⁵ F. D. M. Haldane, Phys. Rev. Lett. 61, 2015 (1988).

⁶ L. Sheng, D. N. Sheng, C. S. Ting, and F. D. M. Haldane, Phys. Rev. Lett. 95, 136602 (2005).

⁷ C. K. Chiu, J. C. Teo, A. P. Schnyder and S. Ryu, Rev. Mod. Phys. 88, 035005 (2016).

⁸ A. P. Schnyder, S. Ryu, A. Furusaki and A. W. Ludwig, Phys. Rev. B 78, 195125 (2008).

⁹ D. J. Thouless, M. Kohmoto, M. P. Nightingale, and M. den Nijs, Phys. Rev. Lett. 49, 405 (1982).

¹⁰ T. Fukui, Y. Hatsugai, and H. Suzuki, J. Phys. Soc. Jpn. 74, 1674 (2005).

¹¹ J. J. Miao, H. K. Jin, F. C. Zhang and Y. Zhou, Phys. Rev. Lett. 118, 267701 (2017).

¹² X. L. Qi, T. L. Hughes and S. C. Zhang, Phys. Rev. B 82, 184516 (2010).

¹³ N. Read and D. Green, Phys. Rev. B 61, 10267 (2000).

¹⁴ X. L. Qi and S. C. Zhang, Rev. Mod. Phys. 83, 1057 (2011).

¹⁵ G. Jotzu, M. Messer, R. Desbuquois, M. Lebrat, T. Uehlinger, D. Greif, and T. Esslinger, Nature (London) 515, 237 (2014).

¹⁶ X. Li, Z. Chen and T. K. Ng arXiv:1903.05013 (2019).